

NEURAL NETWORKS WITH TRAINABLE MATRIX ACTIVATION FUNCTIONS

YUWEN LI, ZHENGQI LIU, AND LUDMIL ZIKATANOV

ABSTRACT. The training process of neural networks usually optimize weights and bias parameters of linear transformations, while nonlinear activation functions are pre-specified and fixed. This work develops a systematic approach to constructing matrix activation functions whose entries are generalized from ReLU. The activation is based on matrix-vector multiplications using only scalar multiplications and comparisons. The proposed activation functions depend on parameters that are trained along with the weights and bias vectors. Neural networks based on this approach are simple and efficient and are shown to be robust in numerical experiments.

1. INTRODUCTION

In recent decades, deep neural networks (DNNs) have achieved significant successes in many fields such as computer vision and natural language processing [1], [2]. The DNN surrogate model is constructed using recursive composition of linear transformations and nonlinear activation functions. To achieve good performance, it is essential to choose activation functions suitable for specific applications. In practice, Rectified Linear Unit (ReLU) is one of the most popular activation functions for its simplicity and efficiency. A drawback of ReLU is the presence of vanishing gradient in the training process, known as dying ReLU problem [3]. Several relatively new activation approaches are proposed to overcome this problem, e.g., the simple Leaky ReLU, and Piecewise Linear Unit (PLU) [4], Soft-plus [5], Exponential Linear Unit (ELU) [6], Scaled Exponential Linear Unit (SELU) [7], Gaussian Error Linear Unit (GELU) [8].

Although the aforementioned activation functions are shown to be competitive in benchmark tests, they are still fixed nonlinear functions. In a DNN structure, it is often hard to determine a priori the optimal activation function for a specific application. In this paper, we shall generalize ReLU and introduce arbitrary trainable matrix activation functions. The effectiveness of the proposed approach is validated using function approximation examples and well-known benchmark datasets such as CIFAR-10 and CIFAR-100. There are a few classical works on adaptively tuning of parameters in the training process, e.g., the parametric ReLU [9]. However, our adaptive matrix activation functions are shown to be competitive and more robust in those experiments.

1.1. Preliminaries. We consider the general learning process based on a given training set $\{(x_n, f_n)\}_{n=1}^N$, where the inputs $\{x_n\}_{n=1}^N \subset \mathbb{R}^d$ and outputs $\{f_n\}_{n=1}^N \subset \mathbb{R}^J$ are implicitly related via an unknown target function $f: \mathbb{R}^d \rightarrow \mathbb{R}^J$ with $f_n = f(x_n)$. The ReLU activation function is a piecewise linear function given by

$$(1.1) \quad \sigma(t) = \max\{t, 0\}, \quad \text{for } t \in \mathbb{R}.$$

In the literature σ is acting component-wise on an input vector. In a DNN, let L be the number of layers and n_ℓ denote the number of neurons at the ℓ -th layer for $0 \leq \ell \leq L$ with $n_0 = d$ and $n_L = J$. Let $\mathcal{W} = (W_1, W_2, \dots, W_L) \in \prod_{\ell=1}^L \mathbb{R}^{n_\ell \times n_{\ell-1}}$ denote the tuple of admissible weight matrices and $\mathcal{B} = (b_1, b_2, \dots, b_L) \in \prod_{\ell=1}^L \mathbb{R}^{n_\ell}$ the tuple of admissible bias vectors. The ReLU DNN approximation to f at the ℓ -th layer is recursively defined as

$$(1.2) \quad \eta_{L, \mathcal{W}, \mathcal{B}} := h_{W_L, b_L} \circ \sigma \circ \dots \circ h_{W_2, b_2} \circ \sigma \circ h_{W_1, b_1},$$

where $h_{W_\ell, b_\ell}(x) = W_\ell x + b_\ell$ is an affine linear transformation at the ℓ -th layer. The traditional training process for such a DNN is to find optimal $\mathcal{W}_* \in \prod_{\ell=1}^L \mathbb{R}^{n_\ell \times n_{\ell-1}}$, $\mathcal{B}_* \in \prod_{\ell=1}^L \mathbb{R}^{n_\ell}$, (and thus optimal $\eta_{L, \mathcal{W}_*, \mathcal{B}_*}$) such that

$$(1.3) \quad (\mathcal{W}_*, \mathcal{B}_*) = \arg \min_{\mathcal{W}, \mathcal{B}} E(\mathcal{W}, \mathcal{B}), \quad \text{where } E(\mathcal{W}, \mathcal{B}) = \frac{1}{N} \sum_{n=1}^N |f_n - \eta_{L, \mathcal{W}, \mathcal{B}}(x_n)|^2.$$

In other words, $\eta_{L, \mathcal{W}_*, \mathcal{B}_*}$ best fits the data with respect to the discrete ℓ^2 norm within the function class $\{\eta_{L, \mathcal{W}, \mathcal{B}}\}$. In practice, the sum of squares norm in E could be replaced with more convenient norms.

2. TRAINABLE MATRIX ACTIVATION FUNCTION

Having a closer look at ReLU σ , we observe that the activation $\sigma \circ \eta_\ell(x) = \sigma(\eta_\ell(x))$ could be realized as a matrix-vector multiplication $\sigma \circ \eta_\ell(x) = D_\ell(\eta_\ell(x))\eta_\ell(x)$ or equivalently $\sigma \circ \eta_\ell = (D_\ell \circ \eta_\ell)\eta_\ell$, where D_ℓ is a *diagonal* matrix-valued function mapping from \mathbb{R}^{n_ℓ} to $\mathbb{R}^{n_\ell \times n_\ell}$ with entries from the discrete set $\{0, 1\}$. This is a simple but quite useful observation. There is no reason to restrict on $\{0, 1\}$ and we thus look for a larger set of values over which the diagonal entries of D_ℓ are running or sampled. With slight abuse of notation, our new DNN approximation to f is calculated using the following recurrence relation

$$(2.1) \quad \eta_1 = h_{W_1, b_1}, \quad \eta_{\ell+1} = h_{W_{\ell+1}, b_{\ell+1}} \circ [(D_\ell \circ \eta_\ell)\eta_\ell], \quad \ell = 1, \dots, L-1.$$

Here each D_ℓ is diagonal and is of the form

$$(2.2) \quad D_\ell(y) = \text{diag}(\alpha_{\ell,1}(y_1), \alpha_{\ell,2}(y_2), \dots, \alpha_{\ell, n_\ell}(y_{n_\ell})), \quad y \in \mathbb{R}^{n_\ell},$$

where $\alpha_{\ell,i}(y_i)$ is a nonlinear function to be determined. Since piecewise constant functions can approximate a continuous function within arbitrarily high accuracy, we choose $\alpha_{\ell,i}$ with $1 \leq i \leq n_\ell$ to be the following step function

$$(2.3) \quad \alpha_{\ell,i}(s) = \begin{cases} t_{\ell,i,0}, & s \in (-\infty, s_{\ell,i,1}], \\ t_{\ell,i,1}, & s \in (s_{\ell,i,1}, s_{\ell,i,2}], \\ \vdots & \\ t_{\ell,i, m_{\ell,i}-1}, & s \in (s_{\ell,i, m_{\ell,i}-1}, s_{\ell,i, m_{\ell,i}}], \\ t_{\ell,i, m_{\ell,i}}, & s \in (s_{\ell,i, m_{\ell,i}}, \infty), \end{cases}$$

where $m_{\ell,i}$ is a positive integer and $\{t_{\ell,i,j}\}_{j=0}^{m_{\ell,i}}$ and $\{s_{\ell,i,j}\}_{j=1}^{m_{\ell,i}}$ are constants. We may suppress the indices ℓ, i in $\alpha_{\ell,i}, m_{\ell,i}, t_{\ell,i,j}, s_{\ell,i,j}$ and write them as α, m, t_j, s_j when those quantities are uniform across layers and neurons. If $m = 1, s_1 = 0, t_0 = 0, t_1 = 1$, then the DNN in (2.1) is exactly ReLU DNN. If $m = 1, s_1 = 0, t_1 = 1$ and t_0 is a fixed small negative number, (2.1) reduces to a DNN based on Leaky ReLU. If $m = 2, s_1 = 0, s_2 = 1, t_0 = t_2 = 0, t_1 = 1$, then $\alpha = \alpha_{\ell,i}$ actually represents the action of a discontinuous activation function.

In our case, we may train the parameters $\cup_{\ell=1}^L \cup_{i=1}^{n_\ell} \{t_{\ell,i,j}\}_{j=0}^{m_{\ell,i}}$ and $\cup_{\ell=1}^L \cup_{i=1}^{n_\ell} \{s_{\ell,i,j}\}_{j=1}^{m_{\ell,i}}$. In such a way, the resulting DNN may use different activation functions for different neurons and layers, and these activation functions are naturally adapted to the target function f (or the target dataset). Since ReLU and Leaky ReLU are included by our DNN as special cases, the proposed DNN is clearly not worse than the traditional ones in practice. In the following, we call the neural network in (2.1), with the activation approach given in (2.2) and (2.3), a DNN based on the ‘‘Trainable Matrix Activation Function (TMAF)’’.

remark. *The activation functions used in TMAF neural network are not piecewise constants. Instead, TMAF activation is realized using matrix-vector multiplication, where entries of those matrices are trainable piecewise constants.*

Starting from the diagonal activation D_ℓ , we can go one step further to construct more general activation matrices. First we note that D_ℓ could be viewed as a nonlinear operator $T_\ell : [C(\mathbb{R}^d)]^{n_\ell} \rightarrow [C(\mathbb{R}^d)]^{n_\ell}$, where

$$[T_\ell(g)](x) = D_\ell(g(x))g(x), \quad g \in [C(\mathbb{R}^d)]^{n_\ell}, \quad x \in \mathbb{R}^d.$$

There seems to be no convincing reason to consider only diagonal operators. A more ambitious possibility is to consider a trainable nonlinear activation *operator* determined by more general matrices, for example, by following tri-diagonal operator

$$(2.4) \quad [T_\ell(g)](x) = \begin{pmatrix} \alpha_{\ell,1} & \beta_{\ell,2} & 0 & \cdots & 0 \\ \gamma_{\ell,1} & \alpha_{\ell,2} & \beta_{\ell,3} & \cdots & 0 \\ \vdots & \ddots & \ddots & \ddots & \vdots \\ 0 & 0 & \cdots & \alpha_{\ell, n_\ell-1} & \beta_{\ell, n_\ell} \\ 0 & 0 & \cdots & \gamma_{\ell, n_\ell-1} & \alpha_{\ell, n_\ell} \end{pmatrix} g(x), \quad x \in \mathbb{R}^d.$$

The diagonal $\{\alpha_{\ell,i}\}$ is given in (2.3) while the off-diagonals $\beta_{\ell,i}, \gamma_{\ell,i}$ are piecewise constant functions in the i -th coordinate y_i of $y \in \mathbb{R}^{n_\ell}$ defined in a fashion similar to $\alpha_{\ell,i}$. Theoretically speaking, even trainable full matrix activation is possible despite of potentially huge training cost. In summary, a DNN based on trainable nonlinear activation operators $\{T_\ell\}_{\ell=1}^L$ reads

$$(2.5) \quad \eta_1 = h_{W_1, b_1}, \quad \eta_{\ell+1} = h_{W_{\ell+1}, b_{\ell+1}} \circ T_\ell(\eta_\ell), \quad \ell = 1, \dots, L-1.$$

	Approximation error			
	Single hidden layer		Two hidden layers	
n	1	2	5	6
ReLU	0.09	0.34	0.14	0.48
Para ReLU	0.04	0.11	0.09	0.47
TMAF	0.01	0.05	0.02	0.13

TABLE 3.1. Approximation errors for $\sin(\pi x_1 + \dots + \pi x_n)$ by neural networks

The evaluation of D_ℓ and T_ℓ are cheap because they require only scalar multiplications and comparisons. When calling a general-purpose packages such as PyTorch or TensorFlow in the training process, it is observed that the computational time of D_ℓ and T_ℓ is comparable to the classical ReLU.

Remark. Our observation also applies to an activation function σ other than ReLU. For example, we may rescale $\sigma(x)$ to obtain $\sigma(\omega_{i,\ell}x)$ using a set of constants $\{\omega_{i,\ell}\}$ varying layer by layer and neuron by neuron. Then $\sigma(\omega_{i,\ell}x)$ are used to form a matrix activation function and a TMAF DNN, where $\{\omega_{i,\ell}\}$ are trained according to given data and are adapted to the target function.

3. NUMERICAL RESULTS

In this section, we demonstrate the feasibility and efficiency of TMAF by comparing it with traditional ReLU-type activation functions. Recall that neurons in the ℓ -th layer will be activated by the matrix D_ℓ . In principle, all parameters in (2.3) are allowed to be trained. To ensure practical efficiency, each diagonal entry $\alpha_\ell = \alpha_{\ell,i}$ of D_ℓ remains the same for all i . We shall only let function values $\{t_{\ell,i,j}\}$ in (2.3) be trained in the following. In each experiment, we use the same learning rates, stochastic optimization methods, and number NE of epochs (optimization iterations). In particular, the learning rate is $1e-4$ from epoch 1 to $\frac{NE}{2}$ and $1e-5$ is used from epoch $\frac{NE}{2} + 1$ to NE. The optimization method is ADAM ([10]) based on mini-batches of size 500. Numerical experiments are performed in PyTorch ([11]). We provide two sets of numerical examples:

- Function approximations by TMAF networks and ReLU-type networks;
- Classification problems for MNIST and CIFAR set solved by TMAF and ReLU networks.

For the first class of examples we use the ℓ^2 -loss function as defined in (1.3). For the classification problems we consider the *cross-entropy* that is widely used as a loss function in classification models. The cross entropy is defined using a training set having p images, each with N pixels. Thus, the training dataset is equivalent to the vector set $\{z_j\}_{j=1}^p \subset \mathbb{R}^N$ with each z_j being an image. The j -th image belongs to a class $c_j \in \{1, \dots, M\}$. The neural network maps z_j to $x_j \in \mathbb{R}^M$,

$$x_j := \eta_{L,\mathcal{W},\mathcal{B}}(z_j) \in \mathbb{R}^M, \quad z_j \in \mathbb{R}^N, \quad j = 1, \dots, p.$$

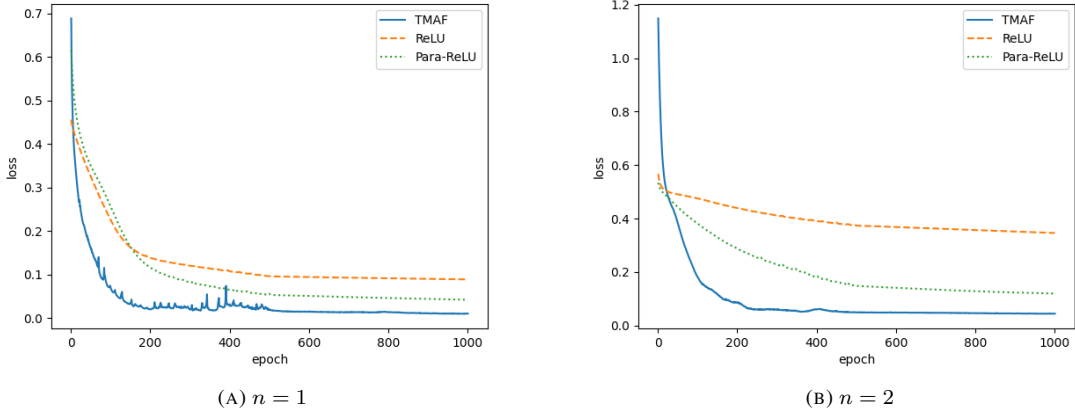
The cross entropy loss function of $\eta_{L,\mathcal{W},\mathcal{B}}$ then is defined by

$$\mathcal{E}(\mathcal{W}, \mathcal{B}) = -\frac{1}{p} \sum_{k=1}^p \log \left(\frac{\exp(x_{c_k,k})}{\sum_{j=1}^M \exp(x_{j,k})} \right).$$

3.1. Approximation of a smooth function. As our first example, we use neural networks to approximate

$$f(x_1, \dots, x_n) = \sin(\pi x_1 + \dots + \pi x_n), \quad x_k \in [-2, 2], \quad k = 1, \dots, n.$$

The training datasets consist of 20000 input-output data pairs where the input data are randomly sampled from the hypercube $[-2, 2]^n$ based on uniform distribution. The neural networks have single or double hidden layers. Each layer (except input and output layers) has 20 neurons. For TMAF D_ℓ in (2.2), the function $\alpha = \alpha_{\ell,i}$ uses intervals $(-\infty, -1.4)$, $(-1.4, -0.92]$, $(-0.92, -0.56]$, $(-0.56, -0.26]$, $(-0.26, 0]$, $(0, 0.26]$, $(0.26, 0.56]$, $(0.56, 0.92]$, $(0.92, 1.4]$, $(1.4, \infty)$ such that probability over each of the ten intervals is 0.1 with respect to Gaussian distribution. Moreover, we apply BatchNorm1d in PyTorch to the linear output of neural networks in each hidden layer. The approximation results are shown in Table 3.1 and Figures 1–2, where Para-ReLU stands for the parametric ReLU neural network. It is observed that TMAF is the most accurate activation approach in these examples.

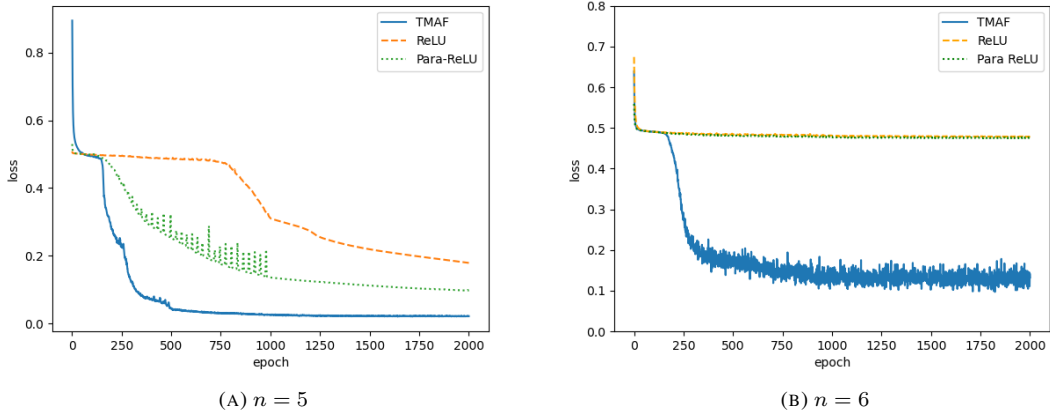
FIGURE 1. Training errors for $\sin(\pi x_1 + \cdots + \pi x_n)$, single hidden layer

3.2. Approximation of an oscillatory function. The next example is on approximating the following function having high, medium and low frequency components

$$(3.1) \quad f(x) = \sin(100\pi x) + \cos(50\pi x) + \sin(\pi x),$$

see Figure 3a for an illustration. In fact, the function in (3.1) is rather difficult to capture by traditional approximation methods as it is highly oscillatory. We consider ReLU, parametric ReLU, and diagonal TMAF neural networks with 3 hidden layers and 400 neurons per layer (except the first and last layers). We also consider the tri-diagonal TMAF (denoted by Tri-diag TMAF, see (2.4)) with 3 hidden layers and 300 neurons per layer. The training datasets are 20000 input-output data pairs where the input data are randomly sampled from the interval $[-1, 1]$ based on uniform distribution.

The diagonal TMAF uses $\alpha = \alpha_{\ell,i}$ in (2.3) with intervals $(-\infty, -1]$, $(-1 + kh, -1 + (k+1)h]$, $(1, \infty)$ for $h = 0.02$, $0 \leq k \leq 99$. The tri-diagonal TMAF is given in (2.4), where $\{\alpha_{\ell,i}\}$ is the same as the diagonal TMAF, while $\{\beta_{\ell,i}\}$ are piecewise constants with respect to intervals $(-\infty, -2.01 + h]$, $\{(-2.01 + kh, -2.01 + (k+1)h)\}_{k=0}^{99}$, $(-0.01, \infty)$, and $\{\gamma_{\ell,i}\}$ are piecewise constants based on $(-\infty, 0.01]$, $\{(0.01 + kh, 0.01 + (k+1)h)\}_{k=0}^{99}$, $(2.01, \infty)$, respectively. Numerical results could be found in Figures 3b, 4, 5 and Table 3.2.

FIGURE 2. Training errors for $\sin(\pi x_1 + \cdots + \pi x_n)$, two hidden layers.

	final loss
ReLU	1.00
Para ReLU	1.00
Diag TMAF	6.45e-2
Tri-diag TMAF	5.81e-2

TABLE 3.2. Error comparison for $\sin(100\pi x) + \cos(50\pi x) + \sin(\pi x)$

For this challenging problem, we note that the diagonal TMAF and tri-diagonal TMAF produce high-quality approximations (see Figures 4 and 3b) while ReLU and parametric ReLU are not able to approximate the highly oscillating function within reasonable accuracy, see Figure 3b and Table 3.2. Moreover, it is observed from Figure 5 that ReLU and parametric ReLU actually approximate the low frequency part of the target function. To capture the high frequency, ReLU-type neural networks are clearly required to use much more neurons, introducing significantly amount of weight and bias parameters. On the other hand, increasing the number of intervals in TMAF only lead to a few more training parameters.

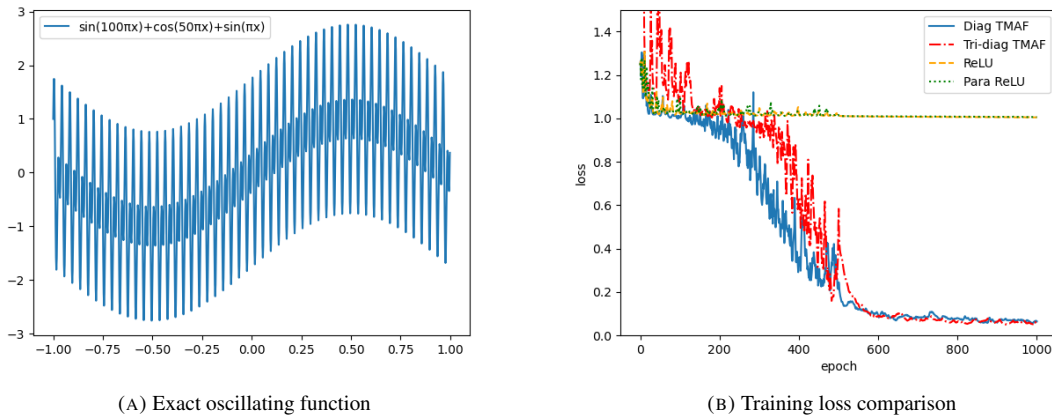


FIGURE 3. Plot of $\sin(100\pi x) + \cos(50\pi x) + \sin(\pi x)$ and training loss comparison

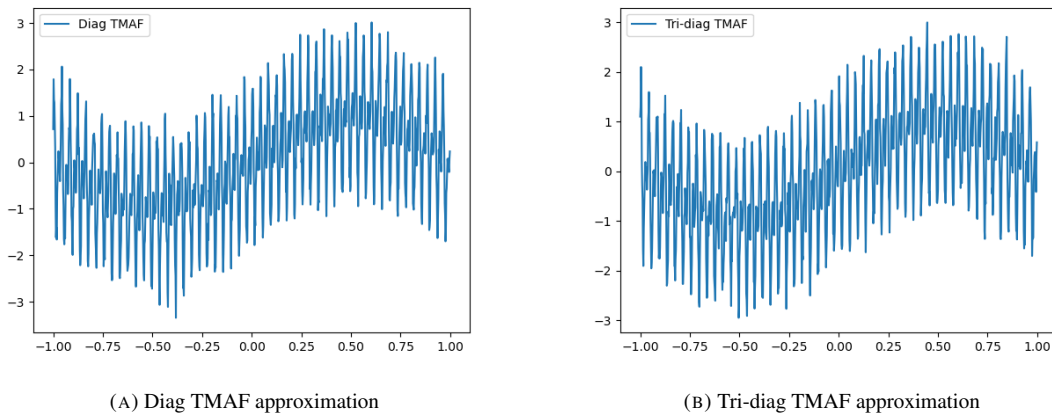


FIGURE 4. Approximations to $\sin(100\pi x) + \cos(50\pi x) + \sin(\pi x)$, TMAF-type

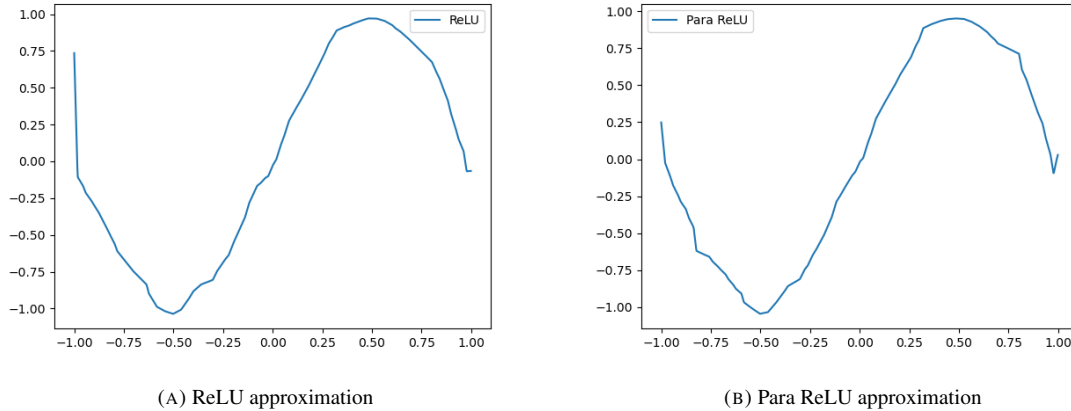


FIGURE 5. Approximations to $\sin(100\pi x) + \cos(50\pi x) + \sin(\pi x)$, ReLU-type

3.3. Classification of MNIST and CIFAR datasets. We now test TMAF by classifying images in the MNIST, CIFAR-10 and CIFAR-100 dataset.

For the MNIST set, we implement double layer fully connected networks defined as in (1.2) and (2.1) with 10 neurons per layer (except at the first layer $n_0 = 764$), and we use ReLU or diagonal TMAF as described in Subsection 3.1. Numerical results are shown in Figures 6a, 6b and Table 3.3. We observe that performance of the TMAF and the ReLU networks are similar. Such a behavior clearly should be expected for a simple dataset such as MNIST.

For the CIFAR-10 dataset, we use the ResNet18 network structure provided by [12]. The activation functions are still ReLU and the diagonal TMAF used in Subsection 3.1. Numerical results are presented in Figures 7a, 7b and Table 3.3. Those parameters given in [11] are already tuned well with respect to ReLU. Nevertheless, TMAF still produces smaller errors in the training process and returns better classification results in the evaluation stage, see Table 3.3.

For the CIFAR-100 dataset, we use the ResNet34 network structure provided by [12] with the ReLU and TMAF activation functions in Subsection 3.1. Numerical results are presented in Figures 8a and 8b. In the training process, TMAF again outperforms the classical ReLU network.

It is possible to improve the performance of TMAF applied to those benchmark datasets. The key point is to select suitable intervals in $\alpha_{\ell,i}$ to optimize the performance. A simple strategy is to let those intervals in (2.3) be varying and adjusted in the training process, which will be investigated in our future research.

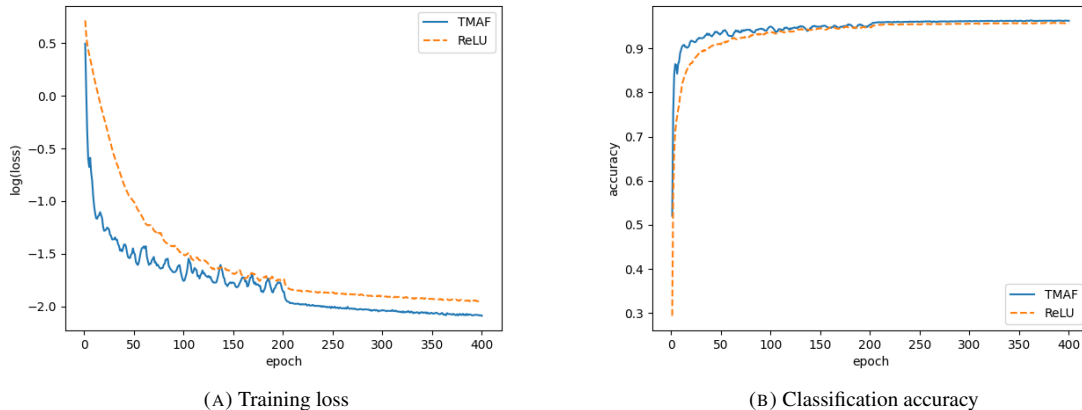


FIGURE 6. MNIST: Two hidden layers

Dataset	Evaluation Accuracy	
	ReLU	TMAF
MNIST (2 hidden layers)	91.8%	92.2%
CIFAR-10 (Resnet18)	77.5%	80.2%

TABLE 3.3. Evaluation accuracy for CIFAR-10

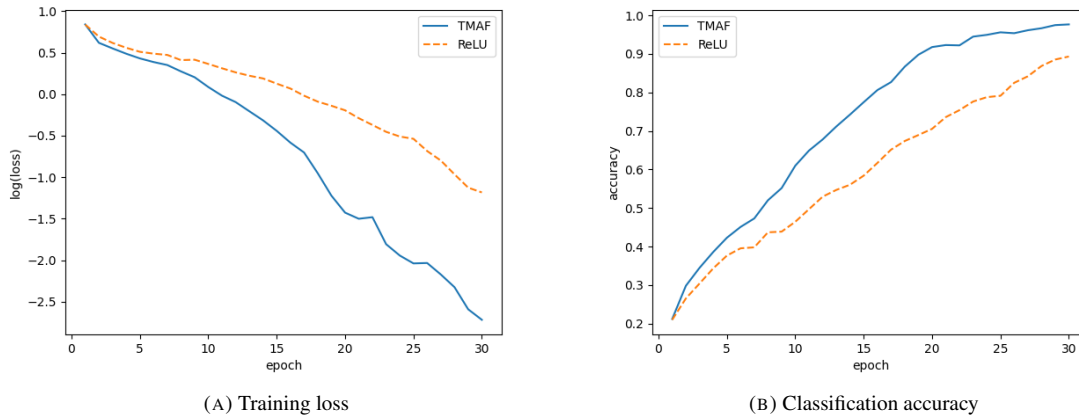


FIGURE 7. Comparison between ReLU and TMAF for CIFAR-10

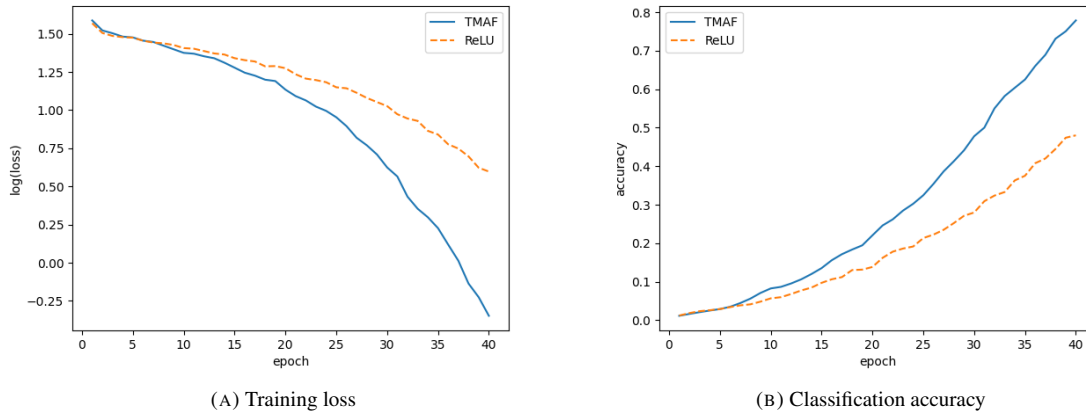


FIGURE 8. Comparison between ReLU and TMAF for CIFAR-100

REFERENCES

- [1] Athanasios Voulodimos, Nikolaos Doulamis, Anastasios Doulamis, and Eftychios Protopapadakis. Deep learning for computer vision: A brief review. *Computational Intelligence and Neuroscience*, 2018:7068349, February 2018.
- [2] Daniel W. Otter, Julian R. Medina, and Jugal K. Kalita. A survey of the usages of deep learning in natural language processing. *arXiv preprint*, arXiv: 1807.10854, 2018.
- [3] Lu Lu, Yeonjong Shin, Yanhui Su, and George E. Karniadakis. Dying relu and initialization: Theory and numerical examples. *arXiv preprint*, arXiv: 1903.06733, 2019.
- [4] Andrei Nicolae. PLU: the piecewise linear unit activation function. *arXiv preprint*, arXiv: 1809.09534, 2018.
- [5] Xavier Glorot, Antoine Bordes, and Yoshua Bengio. Deep sparse rectifier neural networks. In Geoffrey J. Gordon, David B. Dunson, and Miroslav Dudík, editors, *Proceedings of the Fourteenth International Conference on Artificial Intelligence and Statistics, AISTATS 2011, Fort Lauderdale, USA, April 11-13, 2011*, volume 15 of *JMLR Proceedings*, pages 315–323. JMLR.org, 2011.

- [6] Djork-Arné Clevert, Thomas Unterthiner, and Sepp Hochreiter. Fast and accurate deep network learning by exponential linear units (elus). In Yoshua Bengio and Yann LeCun, editors, *4th International Conference on Learning Representations, ICLR 2016, San Juan, Puerto Rico, May 2-4, 2016, Conference Track Proceedings*, 2016.
- [7] Günter Klambauer, Thomas Unterthiner, Andreas Mayr, and Sepp Hochreiter. Self-normalizing neural networks. In Isabelle Guyon, Ulrike von Luxburg, Samy Bengio, Hanna M. Wallach, Rob Fergus, S. V. N. Vishwanathan, and Roman Garnett, editors, *Advances in Neural Information Processing Systems 30: Annual Conference on Neural Information Processing Systems 2017, December 4-9, 2017, Long Beach, CA, USA*, pages 971–980, 2017.
- [8] Dan Hendrycks and Kevin Gimpel. Bridging nonlinearities and stochastic regularizers with gaussian error linear units. *arXiv preprint*, arXiv: 1606.08415, 2016.
- [9] Kaiming He, Xiangyu Zhang, Shaoqing Ren, and Jian Sun. Delving deep into rectifiers: Surpassing human-level performance on imagenet classification. *arXiv preprint*, arXiv: 1502.01852, 2015.
- [10] Diederik P. Kingma and Jimmy Ba. Adam: A method for stochastic optimization. In Yoshua Bengio and Yann LeCun, editors, *3rd International Conference on Learning Representations, ICLR 2015, San Diego, CA, USA, May 7-9, 2015, Conference Track Proceedings*, 2015.
- [11] Adam Paszke, Sam Gross, Francisco Massa, Adam Lerer, James Bradbury, Gregory Chanan, Trevor Killeen, Zeming Lin, Natalia Gimelshein, Luca Antiga, Alban Desmaison, Andreas Kopf, Edward Yang, Zachary DeVito, Martin Raison, Alykhan Tejani, Sasank Chilamkurthy, Benoit Steiner, Lu Fang, Junjie Bai, and Soumith Chintala. Pytorch: An imperative style, high-performance deep learning library. In H. Wallach, H. Larochelle, A. Beygelzimer, F. d'Alché-Buc, E. Fox, and R. Garnett, editors, *Advances in Neural Information Processing Systems*, volume 32. Curran Associates, Inc., 2019.
- [12] Kaiming He, Xiangyu Zhang, Shaoqing Ren, and Jian Sun. Deep residual learning for image recognition. *arXiv preprint*, arXiv: 1512.03385, 2015.

DEPARTMENT OF MATHEMATICS, THE PENNSYLVANIA STATE UNIVERSITY, UNIVERSITY PARK, PA 16802, USA
Email address: yuwenli925@gmail.com, zb15196@psu.edu, ltz1@psu.edu